CONTROLS FEASIBILITY INVESTIGATION WITH A DISCRETE-TIME CFD-BASED SYSTEM IDENTIFICATION ROUTINE

Charles R. O'Neill*
Mechanical and Aerospace Engineering Department
Oklahoma State University
Stillwater, OK 74078

Abstract

A feasibility study investigated the performance of a discrete-time CFD based system identification for a simple wing-flap controls experiment. An analytical model was developed to assist with determining physical sensitivities. Based on this analytical model, a CFD experiment was designed. A controls methodology is reviewed and modified for use with an ARMA aerodynamics model. A discrete-time aerodynamics model was created based on CFD output. Problems with the integration of controls and ARMA models are discussed. The results show that the combined controls and system identification routine is barely operational. The entire controls process appears to be extremely sensitive to system model parameters. Further, the Ricatti method for gain selection appears to have limited practical use.

Nomenclature

$C_{l_{1/4c}}$ = quarter chord moment coefficient
C_{lf} = flap lift coefficient
$C_{l\alpha}$ = lift coefficient slope
D = pivot distance
e = flap/wing chord ratio
I = rotational inertia
k = control gain matrix
L = lift
M = mach number
S = wing area
U = free stream velocity
x = state variable
α = angle of attack
δ = flap deflection
θ = pitch angle

Introduction

This feasibility study investigates system identification control performance for an aeroservoelastic testcase. An analytical model will be created for initial geometry and flow sizing. Next, a CFD representation of the selected geometry will be developed. System identification will be used to develop a discrete-time representation of the aerodynamics. Next, experiments will be conducted in combining the aero-structural model with controls. The objective is to demonstrate aeroservoelasticity with system-identification and to identify possible implementation difficulties.

The general testcase geometry is a two-dimensional wing with a trailing edge control flap. The entire wing is elastically restrained about an upstream rotation point. The generalized geometry is shown in Figure 1.

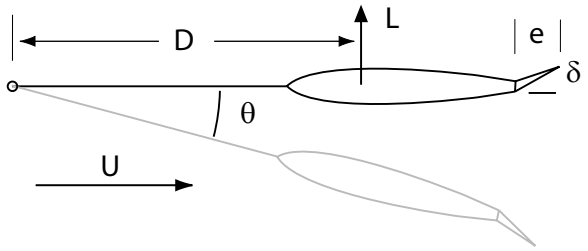

Figure 1 Testcase Geometry

The generalized governing equations describing this geometry were developed through summation of moments around the rotational pivot. The governing equations for rigid body dynamics are simple; the governing equations for aerodynamics are not.

Analytical Controls

A simple analytical controls model was developed to determine geometry and aerodynamics sensitivities. A few simplifying assumptions were used to reduce the complexity of the aerodynamics. First, the overall aerodynamic lift is assumed quasi steady with respect to angle of attack and pitch rate. Second, the flap aerodynamics are assumed to affect lift and pitch moment linearly with the flap angle. Pinkerton[2] provides a simple method for estimating these flap control derivative.

Deriving the governing equation consisted of a moment balance around the pivot point. Combining the balance with the aerodynamics yields Equation (1).

* Graduate Research Assistant, Student Member AIAA.

$$
\begin{aligned}
I\,\ddot{\theta} &= -DL + M \\
L &= q\,S\left(C_{l\alpha}\cdot\alpha + e\,\frac{dC_{lf}}{d\delta}\,\delta\right) \\
M &= qSc\left(C_{m_{1/4c}} + \frac{dC_m}{d\delta}\,\delta\right)
\end{aligned}
\tag{1}
$$

Additionally, the airfoil angle of attack is specified through geometry in Equation (2).

$$
\begin{aligned}
\alpha &= \theta + \arctan\left(\frac{\dot{\theta}D}{U}\right) \\
&\approx \theta + \frac{\dot{\theta}D}{U}
\end{aligned}
\tag{2}
$$

The second order differential equation in θ with a control input δ is given in Equation (3). For a symmetrical airfoil, D is zero.

$$
\begin{aligned}
\ddot{\theta} &= A\dot{\theta} + B\theta + C\delta + D \\
A &= -\frac{q\,S\,D}{I}\cdot\frac{C_{l\alpha}}{\sqrt{1-M^2}} \\
B &= -\frac{q\,S\,D^2}{I\,U}\cdot\frac{C_{l\alpha}}{\sqrt{1-M^2}} \\
C &= \frac{q\,S}{I}\left(\frac{dC_m}{d\delta} - D\cdot e\cdot\frac{dC_{lf}}{d\delta}\right) \\
D &= \frac{q\,S}{I}\cdot C_{l_{1/4c}}
\end{aligned}
\tag{3}
$$

Conversion to state space form is straightforward and is given in Equation (4). The state vector is $\vec{x} = [\alpha \quad \dot{\alpha}]^T$.

$$
\dot{\vec{x}} = \begin{bmatrix} 0 & 1 \\ A & B \end{bmatrix}\vec{x} + \begin{bmatrix} 0 \\ C \end{bmatrix}\delta \tag{4}
$$

A MathCAD document was written to investigate sensitivities and initial control algorithms. Equation (2) is converted to discrete state space form with the relevant geometry and aerodynamic parameters and a solution is found by time-marching forward.

Experimentation and intuition was used to size parameters. Because CFD solutions are expensive, this initial sizing was important to be able to select a useful and realizable geometry for the later CFD training runs. Difficulties were found in selecting ratios of inertia, I, and pivot distance, D, which met the following criteria. First, low open-loop damping was desired so that a difference could be seen between the open loop and closed loop systems. Second, high oscillation frequency was desired to improve the ARMA system model's performance.

However, initial experimentation found that damping geometry is sensitive to pivot distance, D. A comparison with the governing equation shows that frequency increases with the square root of pivot distance and damping increases with the 3/2 power of pivot distance. Large pivots provide vastly too much damping for the wanted increase in frequency. The final parameters are based on a high velocity flow with a compromised pivot distance. The open loop response to an input flap disturbance is show in Figure 2. The natural frequency is 33 Hz with a damping ratio of 13 percent.

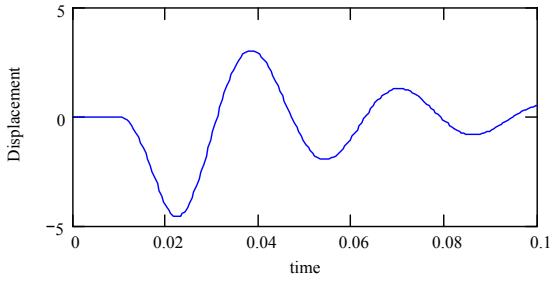

Figure 2 Open Loop Response

The first control system to be investigated was the eigenvalue placement method. For this method, an augmented plant matrix was derived based on state feedback into the flap control angle. Control gains result from the specification of the system's frequency and damping ratio. On initial inspection, this method appears to be superior, however, the control gains selected often result in tremendous control inputs being applied. As the eigenvalues selected become further away from the natural system's, the gains increase. For example, keeping the same frequency and increasing the damping to 0.707 yields the following response shown in Figure 3. Notice that for an initial offset of 10 degrees, the flap deflection angle approaches 40 degrees. This response probably has violated the flap-angle assumptions in the model.

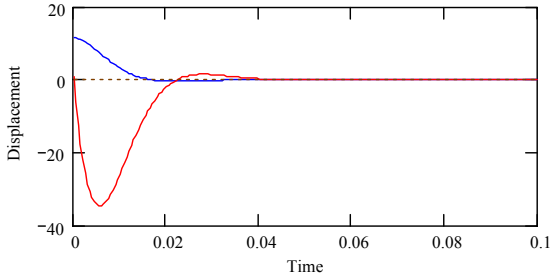

Figure 3 Eigenvalue Placement

The next control system is based on the Riccati method of selecting control gains. For this method, the gains are found by solving the Ricatti equation with the appropriate effective limitations on control inputs and state outputs. For an input limitation of 23 degrees and an output limitation of 5 degrees, Ricatti control gain matrices are shown in Equation (5)

$$Q = \begin{bmatrix} \frac{1}{0.1^2} & 0 \\ 0 & 0 \end{bmatrix} \qquad (5)$$
$$R = \begin{bmatrix} \frac{1}{0.4^2} \end{bmatrix}$$

The resulting control gains are k={-1.248, -0.013}. These gains produced the response in Figure 4.

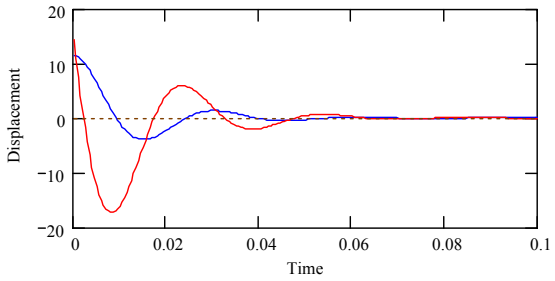

Figure 4 Ricatti Control Response

This analytical experiment does not apply system identification to controls; however, it allowed an effective combination of geometry and fluid flow to be found for the CFD based control portion of this paper.

CFD Based ARMA Controls

Now, CFD based system identification will be used to develop and evaluate a controls algorithm for the single degree of freedom testcase. Unfortunately, compared to the simple analytical experiment performed above, the CFD based controls is significantly more complicated. This paper will not discuss the ARMA model creation. Only the resulting system model will be used.

Derivation of the appropriate CFD based control algorithm for system identification is described in Gupta[3]. However, the current ARMA implementation has introduced a sign change for the aerodynamics. Following the Gupta's derivation and making the relevant sign changes yields the state-space form for the coupled aeroservoelastic system given in Equation (6). For a gain of zero, this yields the aeroelastic state-space form used in the asemdl3d program.

$$\begin{bmatrix} x_s(k+1) \\ x_a(k+1) \end{bmatrix} = \begin{bmatrix} G_s + q_\infty H_s D_a C_s + q_\infty H_s D_a K C_s & q_\infty H_s C_a \\ H_a C_s - H_a K C_s & G_a \end{bmatrix} \begin{bmatrix} x_s(k) \\ x_a(k) \end{bmatrix} + \begin{bmatrix} q_\infty H_s D_a & q H_s \\ H_a & 0 \end{bmatrix} \begin{bmatrix} q_1 \\ f_1 \end{bmatrix} + \begin{bmatrix} q H_s \\ 0 \end{bmatrix} [f_0] \qquad (6)$$

Also, the derivation in Gupta assumed that only the displacements observable. This creates a gain matrix based only on displacements. For the Ricatti equation to even be applicable, all of the states need to be included. The solution is to include velocity states in the output. This is accomplished by augmenting Gupta's C_s matrix with the appropriate diagonal identity matrices. Also, the H_a and D_a matrices must be augmented with zeros to be compatible with the new output vector. The state-space output equation is given in Equation (7).

$$q = [[C_s][0]] \begin{bmatrix} x_s(k) \\ x_a(k) \end{bmatrix} \qquad (7)$$

Now, the ARMA based aeroservoelastic form is consistent with the current system identification routine.

The first step with CFD was to create a representation of the flow geometry. A NACA 0012 airfoil testcase was selected. The CFD grid is given in Figure 5. Significant refinement occurs aft of the airfoil. This was done to capture the aerodynamics resulting from the shed wake. The grid contains 235-thousand elements.

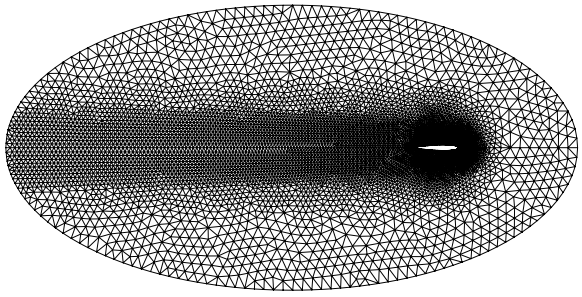

Figure 5 CFD Grid

Next, modeshapes corresponding to the wing rotation and the flap control mode were created with transpiration. The modeshapes are not easily visualized and are not presented. Both the wing rotation and flap deflection modeshapes have a unit deflection of 1 degree.

Aerodynamic training data was generated in parallel with the offset dc-chirp. The chirp frequency swept from zero to 10 percent of Nyquist. Each of the two modes was individually excited to generate the following two training time histories. Figure 6 shows the training time history for the first mode, rotation angle. The figure displays displacement, velocity and two modal forces.

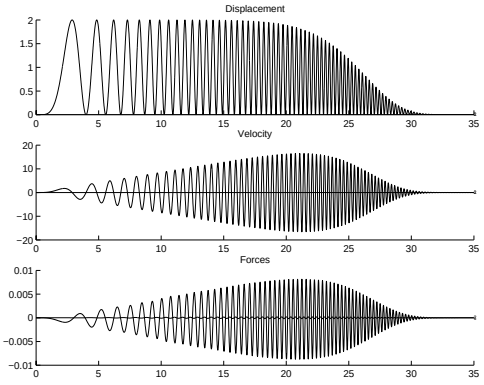

Figure 6 Training Signal Mode1

Interestingly, the force for the first mode is dominated by velocity. Second mode forces are almost hidden by the order of magnitude larger first mode forces; however, the training signal did excite forces in both modes.

Training for mode two is shown in Figure 7. Again, the chirp was swept to 10 percent of Nyquist. The resulting forces due to second mode excitation include more complex aerodynamics than the first mode. The smaller magnitude symmetrical output force is the second mode. The flap produces a symmetrical hinge moment dominated by velocity. Wing moment produced by the flap is clearly dominated by flap displacement, however, velocity effects are also apparent. Interestingly, a bump in output force occurs between time 5 and 15. From the unsteady pressure visualization, it was noticed that the chirp was generating pressure waves moving upstream. This bump in the force plot might represent an unsteady pressure distribution effect similar to the Sears problem.

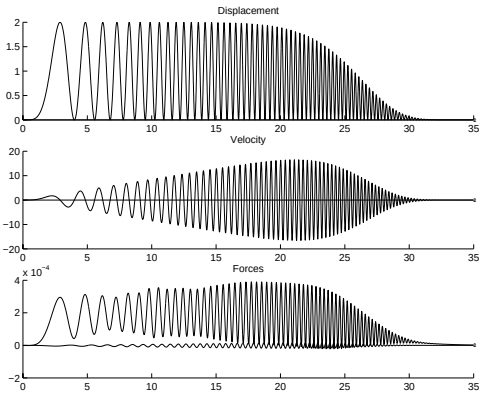

Figure 7 Training Signal Mode 2

Using the training data, multiple ARMA models were generated. Based on the forced response results, a 6-20 model was selected.

Next, an aeroelastic response comparison was made between the traditional asemdl3d code and the matlab code for a control gain of zero. Both routines calculated the same discrete-time plant matrix. However, asemdl3d and matlab gave different eigenvalues for identical input.

From the Matlab documentation[4], the eigenvalue condition number of a matrix is the reciprocal of the cosine of the angle between the left and right eigenvalues. Large condition numbers indicate the possibility of multiple eigenvalue solution sets. For the SDOF testcase, the condition numbers for the structure are 10 and 31. The condition numbers for the coupled aero-structural plant matrix include values from 10^4 to 10^{15}. For these condition numbers, the distinction between individual eigenvalues is so small that the solution method seems to strongly influence the results.

Unfortunately, this problem dominates for eigenvalues near the real axis. For this testcase, the almost-rigid-body characteristics create low frequencies for the system identification sample rate. This sample rate problem also made free response calculation require thousands of timesteps.

Another eigenvalue problem occurs because of poor model frequency response. In this case, the aerodynamics create an eigenvalue near the unit circle. The following example illustrates some of the problem encountered with a purely numerical eigenvalue that approaches the unit circle. The z plane eigenvalue plot is given in Figure 8. Notice that the unwanted eigenvalue lies slightly inside the unit circle at approximately 30 percent of the Nyquist frequency. As the dynamic pressure increases, the unwanted eigenvalue drifts further away from the origin.

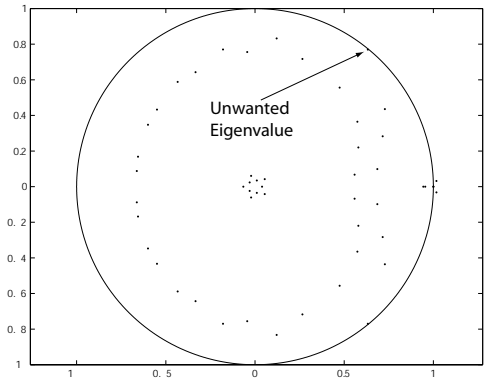

Figure 8 Eigenvalues

Next, the time history is plotted in Figure 9. The interesting part of this figure is the force response shown in the bottom subplot. A pulse force input yields an oscillating force response at the unwanted eigenvalue's frequency. For simple aeroelastic

examples, this is not a fatal problem. The 2nd order structural system filters out the high frequency force components. Unfortunately, using this system model for controls encounters difficulties due to the chattering input force response.

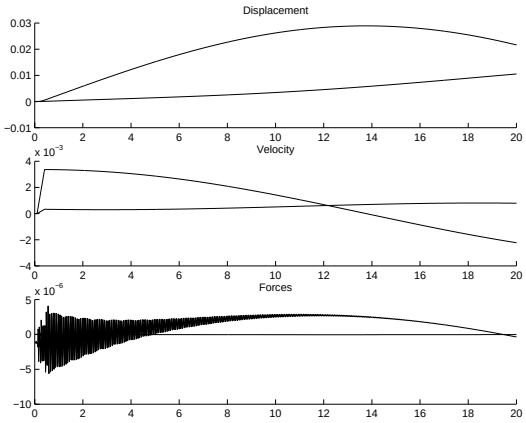

Figure 9 Time history

The Ricatti method for control gain selection was investigated for this testcase. System identification and the Ricatti method do not automatically mesh smoothly. Ricatti assumes state feedback. In the ARMA model, the states contain aerodynamic forces, which are not available in reality. Those tempted to use a state observer will also encounter difficulties because the overall ARMA model is controllable but not observable. This is analogous to not being able to deduce a unique flow field from previous motions. The Ricatti method does not appear to be a good choice for determining control gains with an ARMA model.

In spite of these problems, the Ricatti method was used to find control gains for the SDOF testcase. The Q matrix from the analytical experiment was used; however, the Ricatti solution requires a positive definite R matrix. This requirement forced the R matrix to contain limitation data for all inputs, not just the desired flap deflection angle. To alleviate this problem, the R matrix weighting for non-flap inputs were set to large magnitudes. Thus, the final 22x6 gain matrix only applied inputs into the flap deflection angle. Figure 10 shows the absolute value of the gains for the couple aero-elastic state vector as determined with the Ricatti solution method. The motion gains are:

k={2.029, 0.13197, 0.12102, 0.00783}

So, the flap deflection input would be:

$$\delta_{input} = 2.03 \cdot \theta_{wing} + 0.132 \cdot \delta_{flap} + 0.121 \cdot \dot{\theta}_{wing} + 0.008 \cdot \dot{\delta}_{flap} \quad (8)$$

Notice, the motion terms are well behaved. Flap angle inputs are dominated by the wing pitch angle. The control gains for the actual flap angle is an order of magnitude smaller than wing angle. This is expected and was seen before in the analytical Ricatti solution above. However, the aerodynamic gains are problematic. First, it would be preferred if these gains were zero. Second, the gains have large differences in magnitude with oscillating phase. This indicates an unusually large sensitivity to the aerodynamics.

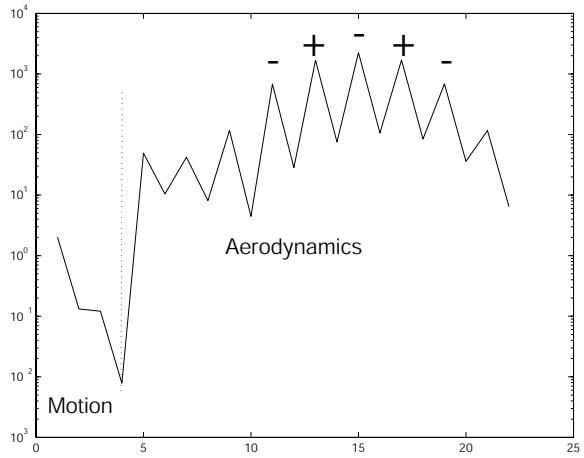

Figure 10 Ricatti Gains

Overall, the Ricatti method for gain determination does not work well with the ARMA system model. To even find a solution, several questionable modifications were made to the standard Ricatti approach. Regardless of theses modifications, the resulting gains still contain fundamental errors when coupled with the ARMA system model.

The control gain selection method that did work was the guess-and-test method. The open loop system was made to dynamically diverge by adjusting dynamic pressure. The open loop time history response is given in Figure 11.

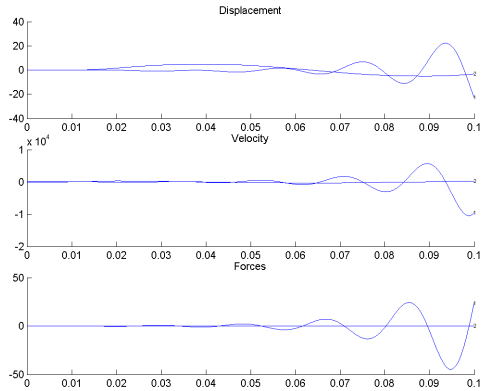

Figure 11 Open Loop Time history

Now, the control scheme is applied to the system. It required many iterations to determine and the optimize the control gains to obtain a stable system. The system was made stable with the following gains.

k={3.5, 0, -0.01, -0.04}

A time history response is given in Figure 12. Although it was not intuitive at first, the better performing control gains included positions and rates of the flap control surface.

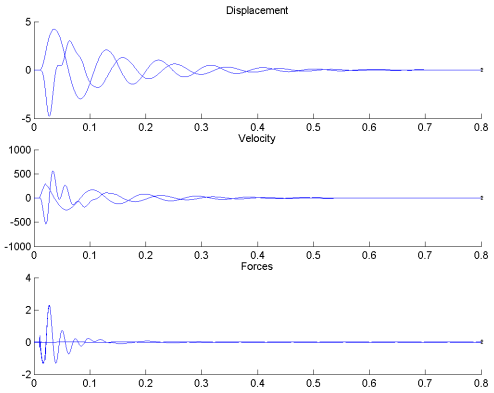

Figure 12 Closed Loop Time history

The unwanted eigenvalue problem surfaced often with the controlled system especially when rates were used in the control gains. The following shows a system made stable with the control gains; however, the unwanted eigenvalues eventually cause non-physical dynamic divergence. The gains are:

k={3.5, 0, -0.01, -0.05}

Notice the small change in gains compared to the previous problem. The time history and eigenvalues are given in Figure 13 and Figure 14. Clearly, the control method is working but the aerodynamic system model fails to accurately represent reality.

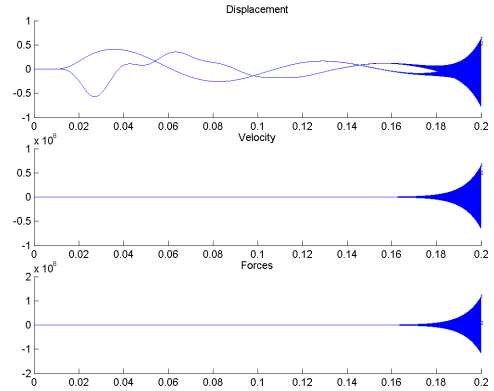

Figure 13 Closed Loop Chatter Time history

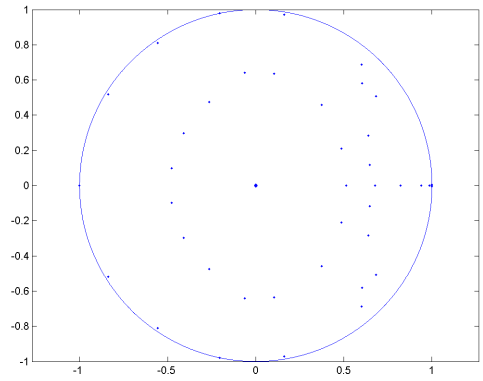

Figure 14 Closed Loop Chatter Eigenvalues

Conclusions and Recommendations

An investigation into system identification coupled with controls was conducted. A successful analytical example was developed for both eigenvalue placement and Ricatti gain selection. Unfortunately, a controls implementation with system identification turned out to be non-trivial and unsuccessful. This is in spite of the simple system algorithm used for the theoretical controls development. Sensitivities were encountered with the eigenvalue calculation routines. Additional sensitivities were encountered with unwanted eigenvalues causing chattering and singing solutions even with the relatively simple aeroelastic results. The ratio in model quality required between aeroelastic and aeroservoelastic appears to be significant. Time scale issues created problems for both simulation lengths and system model sensitivities. Low frequencies produce high eigenvalue sensitivities. The Ricatti method for gain determination does not couple well with the ARMA system identification routine. The control gains that did work properly were selected based on iteration and system response intuition.

In hindsight, the selected testcase geometry was a poor choice. The testcase is sensitive to geometry and does not provide robust dynamics specification. Also, timescale issues created significant problems in solution lengths. Using a rigid body testcase was not a good first investigation testcase. One initial reason for selecting the wing/flap testcase was to experiment with an aft mounted rotation point for divergence prevention. From the analytical results, aft mounting is extremely difficult to control. An initial idea of controlling a wing with a hinge pivot point behind the quarter chord was scrapped after investigating the complications.

This investigation found multiple areas in the system identification routine that need to be either

reevaluated or investigated further. The following recommendations are suggested.

Previous work with the old STARS version of ARMA produced several documents regarding the integration of ARMA with structures and controls. These documents are obsolete with the new Euler3d version of ARMA and need to be revised. In particular, there are sign changes in the coupled aero-structural plant matrices and in the offset forces. This should be a priority because of the implications to information transfer with Dryden and AES.

The asemdl3d program is reporting different eigenvalues than both Matlab and MathCad for the same aeroelastic plant matrices. The discrepancies seem to appear primarily in the imaginary parts of eigenvalues near the real axis. Unfortunately, these eigenvalues are important for aeroelasticity.

References

1. Nelson, R. C., *Flight Stability and Automatic Control,* McGraw-Hill, Boston, 1998.

2. Pinkerton, R. N., "Analytical Determination of the Load on a Trailing Edge Flap," NACA TN-353, October 1930.

3. Gupta, K. K., "STARS - An Integrated, Multidisciplinary, Finite-Element, Structural, Fluids, Aeroelastic, and Aerservoelastic Analysis Computer Program," NASA TM-4795, April 2001.

4. *Matlab6.5 Documentation,* The Mathworks, 2002.